Astron. Astrophys. 221, 146–154 (1989)

ASTRONOMY AND ASTROPHYSICS

Chaotic dynamics of comet Halley

B.V. Chirikov and V.V. Vecheslavov

Institute of Nuclear Physics, 630090 Novosibirsk, USSR

Received August 17, 1987; accepted December 14, 1988

Summary. A simple model of the dynamics of Halley's comet is developed, and its motion is shown to be chaotic due to the perturbations by Jupiter. Estimates for the error growth in the extrapolation of the comet's trajectory are obtained which particularly explain a sharp divergence of different extrapolations of comet Halley's orbit previously obtained. Various mechanisms limiting the full sojourn time of the comet in the solar system are considered. These include the orbit diffusion under the perturbations by Jupiter and by Saturn, the orbit drift due to weak nongravitational forces as well as the prompt ejection of the comet from the solar system upon its very close encounter with Jupiter. The estimated sojourn time of comet Halley in the solar system ($t \sim 10$ Myr) is compared to the period of hypothetical comet showers from the Oort cloud which is about 30 Myr.

Key words: comets – celestial mechanics – chaotic dynamics

1. Introduction

Celestial mechanics, i.e. the dynamics of the solar system, has been always a perfect example of the regular, deterministic, motion which allows a long-term prediction to a fairly high accuracy. Yet, as in almost any other many-dimensional nonlinear oscillator system, the motion of a qualitatively different nature is possible here. We mean the so called dynamical chaos when a trajectory becomes random, i.e. highly irregular and unpredictable, irrespective of any noise (see, e.g., Lichtenberg and Lieberman, 1983; Zaslavsky, 1985). Moreover, according to Arnold's conjecture (Arnold, 1964), which has been well confirmed in numerical experiments (Lichtenberg and Lieberman, 1983; Chirikov, 1979), the chaotic components of motion for the special initial conditions of a positive measure is a generic phenomenon in nonlinear oscillations. The origin of chaos lies in a neighborhood of any separatrix, the trajectory with zero frequency of the unperturbed motion.

In celestial mechanics the simplest example of separatrix is the parabolic trajectory in the two-body problem which separates the bounded and unbounded motions. As is well known by now (Lichtenberg and Lieberman, 1983; Zaslavsky, 1985; Chirikov, 1979), in this case any perturbation, particularly, a regular one, by a uniformly rotating third body, for instance, produces a finite chaotic layer at the side of unperturbed elliptic trajectories. This has been explicitly shown in a recent paper of Petrosky (1986) for a particular case of the plane circular restricted three-body problem.

The orbits close to parabolic, i.e. ones of a large eccentricity $\varepsilon \to 1\,(0 < 1-\varepsilon \ll 1)$, are typical for comets, those "test particles" in celestial mechanics. The most detailed observational data exist for comet Halley due to the various historical records dating back to the year -239 (240 B.C.). The analysis of these data allowed us to conclude that the motion of Halley's comet is chaotic. We present some of its statistical characteristics, particularly, the diffusion rate in energy, the estimates for the comet's life time in the solar system, and the increment of its motion local instability which sets the limit for the extrapolation of comet's trajectory in both directions of time.

Our analysis is based upon the construction of a simple 2-dim. model (a map) for the comet's dynamics, and on the subsequent study of this model by means of the modern theory of dynamical systems.

The motion of comet Halley is a new example of dynamical chaos in celestial mechanics. For earlier studies of chaos in celestial mechanics see, e.g. Everhart, 1979; Wisdom, 1980; Froeschle and Scholl, 1981; Wisdom et al., 1983. A general discussion of the dynamics of comets, chaos included, is presented in a recent paper by Sagdeev and Zaslavsky (1987). Interesting data on unusual motion of the third Soviet spacecraft are given by Gontkovskaja and Chebotarev (1964); they look very irregular and were, apparently, also chaotic.

Extensive numerical simulations of the dynamics of Halley's comet (Yeomans and Kiang, 1981; Kalyuka et al., 1985; Landgraf, 1986) are a striking illustration of the difficulties and limitations in predicting chaotic motion (see Sect. 4 below).

2. The model

The strong instability of a chaotic trajectory restricts its extrapolation to a relatively short time interval irrespective of the modelling accuracy. On the other hand, for studying statistical properties of the motion, one can use a relatively simple model which includes the essential part of dynamics of the real system. In the problem under consideration, we assume it to be the dynamics of the phase of perturbations of the comet by Jupiter. As a conjugate variable it is convenient to choose some quantity proportional to the comet's energy which determines the period of its motion and, hence, a change in the perturbation phase.

In constructing the model we have used, as the original input data, 46 values of t_n, the comet's perihelion passage time, as presented by Yeomans and Kiang (1981) and repeated in Table 1 (t_1 value after Kalyuka et al., 1985). The values for t_n cover a fairly

Send offprint requests to: B. Chirikov

Table 1. Comet Halley's dynamics: perihelion passage times (after Yeomans and Kiang, 1981)

n	Year	Perihelion passage, t_n (JD)	Jupiter's phase X_n	Saturn's phase Y_n
1	1986	2446470.9518[a]	0.	0.
2	1910	2418781.6777	6.39083584	2.57350511
3	1835	2391598.9387	12.6647606	5.09993167
4	1759	2363592.5608	19.1287858	7.70290915
5	1682	2335655.7807	25.5767473	10.2994180
6	1607	2308304.0406	31.8896785	12.8415519
7	1531	2280492.7385	38.3086791	15.4263986
8	1456	2253022.1326	44.6490451	17.9795802
9	1378	2224686.1872	51.1891362	20.6131884
10	1301	2196546.0819	57.6840264	23.2285948
11	1222	2167664.3229	64.3500942	25.9129322
12	1145	2139377.0609	70.8789490	28.5420157
13	1066	2110493.4340	77.5454480	31.2265267
14	989	2082538.1876	83.9976717	33.8247519
15	912	2054365.1743	90.5001572	36.4432169
16	837	2026830.7700	96.8552482	39.0023280
17	760	1998788.1713	103.327633	41.6086720
18	684	1971164.2668	109.703382	44.1761014
19	607	1942837.9758	116.241244	46.8088124
20	530	1914909.6300	122.687259	49.4045374
21	451	1885963.7491	129.368127	52.0948344
22	374	1857707.8424	135.889745	54.7210039
23	295	1828915.8984	142.535083	57.3969935
24	218	1800819.2235	149.019949	60.0083634
25	141	1772638.9340	155.524114	62.6275046
26	66	1745189.4601	161.859602	65.1787221
27	−11	1717323.3485	168.291253	67.7686629
28	−86	1689863.9617	174.629030	70.3208017
29	−163	1661838.0660	181.097560	72.9255932
30	−239	1633907.6180	187.544060	75.5215136
31	−314	1606620.0237	193.842186	78.0576857
32	−390	1578866.8690	200.247766	80.6371280
33	−465	1551414.7388	206.583867	83.1885924
34	−539	1524318.3270	212.837867	85.7069955
35	−615	1496638.0035	219.226637	88.2796687
36	−689	1469421.7792	225.508291	90.8092075
37	−762	1442954.0301	231.617192	93.2691812
38	−835	1416202.8066	237.791521	95.7555018
39	−910	1388819.7203	244.111687	98.3005491
40	−985	1361622.0640	250.389054	100.828362
41	−1058	1334960.1638	256.542767	103.306381
42	−1128	1309149.3447	262.500045	105.705298
43	−1197	1283983.7325	268.308406	108.044248
44	−1265	1259263.8959	274.013879	110.341767
45	−1333	1234416.0059	279.748908	112.651187
46	−1403	1208900.1811	285.638100	115.022687

[a] After Kalyuka et al., 1985.
Effective periods for Jupiter 4332.653; for Saturn 10759.362 (days).

large interval in time from 1986 back to −1403 yr. Notice that only 27 values ($n=2-28$) are reconciled with the observations while the remaining 18 ones ($n=29-46$) have been predicted from the numerical orbit simulations of the comet (Yeomans and Kiang, 1981).

Define the global perturbation phase via Jupiter's position, with respect to the comet's orbit, at a perihelion passage time:

$$X_n = \frac{t_n}{P_J} \tag{1}$$

and set $X_1=0$ (Table 1). Jupiter is assumed to move uniformly in a circular orbit with an effective period $P_J=4332.653$ days. As a matter of fact, P_J includes various perturbations, particularly, Jupiter's and the comet's orbit precession. The above P_J value has been empirically adjusted from the best intrinsic agreement of the original t_n data (see below). Measured in years, P_J is close to the ratio of the Earth's and Jupiter's mean motions.

The comet's period is $P_n=t_n-t_{n-1}$. Define a quantity

$$w_n = \left(\frac{P_n}{P_J}\right)^{-2/3} = (X_n - X_{n-1})^{-2/3} \approx -2E_n \tag{2}$$

where E_n is the comet's total energy, far from Jupiter, within the interval (t_{n-1}, t_n). We set Jupiter's velocity and radius of the orbit to be unity while its mass $\mu_J=9.54\times10^{-4}$ in solar units is the small perturbation parameter. The time unit is then $P_J/2\pi$ $=689.563$ days $=1.888$ years.

The change in w (per comet's period) depends on the perturbation phase $x=X(\mathrm{mod}\ 1)$. Together with Eq. (2) it leads to a canonical map of the plane (w, x) (cf. Petrosky, 1986)

$$w_{n+1} = w_n + F(x_n); \quad x_{n+1} = x_n + w_{n+1}^{-3/2} \tag{3}$$

Apparently, it is the simplest (very restricted though) model of the dynamics of the comet (backwards in time).

The unknown perturbation function $F(x)$ can be found directly from the original data t_n (Table 1) using the same Eq. (3). The result is depicted in Fig. 1. The scattering of points turned out to be caused by the perturbation due to Saturn.

The two perturbations can be separated as follows: let us approximate the dependence in Fig. 1 by a Fourier series $F_J(x)$ and plot the difference $F(x_n)-F_J(x_n)$ vs. Saturn's phase y $=Y(\mathrm{mod}\ 1)$ where $Y=r_S X$ (Table 1), and $r_S=0.4026868$ is Saturn's revolution frequency. The latter has been also empirically adjusted and it turned out to be equal to the ratio of Saturn's and Jupiter's mean motions. The difference $F-F_J$ as a function of y was again approximated by another Fourier series $F_S(y)$, and the whole procedure repeated for the function $F(x_n)-F_S(y_n)$ instead of the initial $F(x_n)$. After about 10 such successive approximations the following decomposition of the total perturbation into that by Jupiter, and by Saturn has been obtained (Fig. 2):

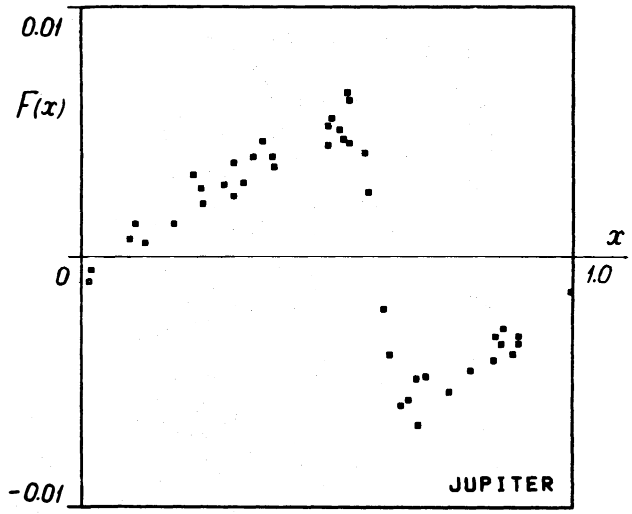

Fig. 1. The full perturbation of comet Halley vs. Jupiter's phase

$$F(x) = F_J(x) + F_S(y) + F_R(z). \tag{4}$$

The final Fourier spectrum of the perturbation is shown in Table 2 where

$$F_J(x) = \sum_m \left[a_m \cos(2\pi m x) + b_m \sin(2\pi m x)\right]$$

for Jupiter, and similarly for Saturn. The mean values $\langle F\rangle \equiv a_0 \equiv 0$ were put equal to zero for both planets because the

Table 2. Perturbation Fourier spectrum in model (3)

	Jupiter			Saturn		
m	$a_m\times10^2$	$b_m\times10^2$	$\sqrt{a_m^2+b_m^2}\times10^2$	$a_m\times10^3$	$b_m\times10^3$	$\sqrt{a_m^2+b_m^2}\times10^3$
0	0	0	0	0	0	0
1	−0.240980	0.390305	0.458704	0.539282	0.402058	0.672663
2	0.182350	−0.060684	0.192182	−0.365971	0.094560	0.377990
3	−0.120144	−0.025157	0.122749	0.055456	−0.195876	0.203575
4	0.053170	0.062750	0.082247	0.087232	0.145022	0.169236
5	−0.002350	−0.051279	0.051333	−0.076651	0.043299	0.088035
6	−0.019543	0.033955	0.039178	−0.019011	−0.032018	0.037237
7	0.019810	−0.006757	0.020931	−0.010290	0.049478	0.050537
8	−0.016521	−0.005454	0.017398	−0.067932	0.063112	0.092724
9	0.003908	0.009710	0.010467	−0.000503	0.012022	0.012033
10	−0.001400	−0.005662	0.005833	0.013116	0.013741	0.018996

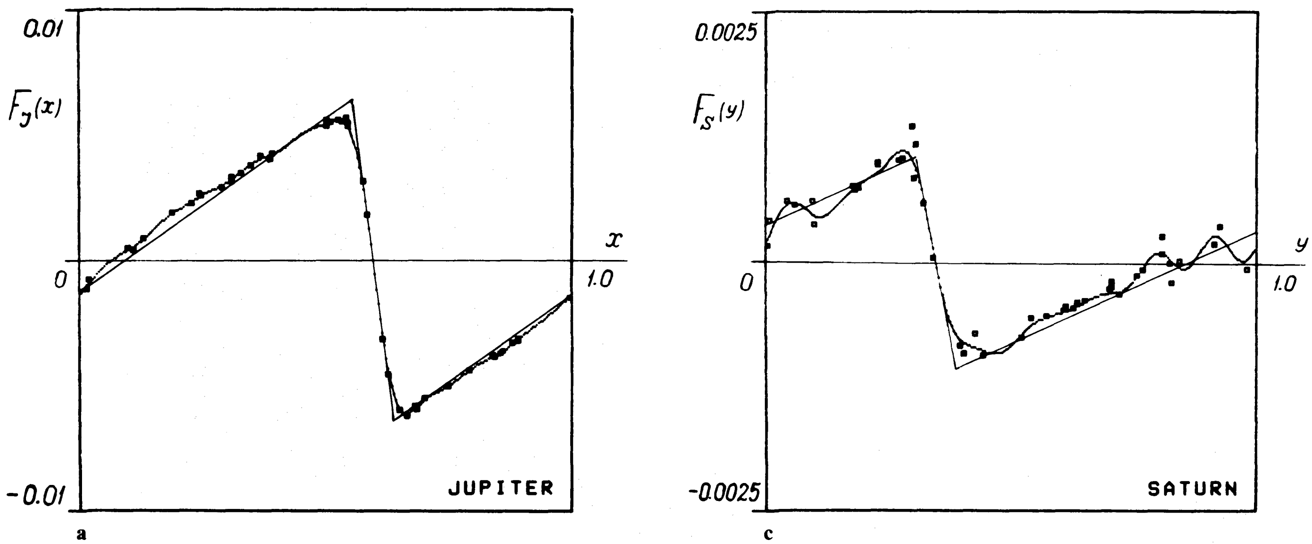

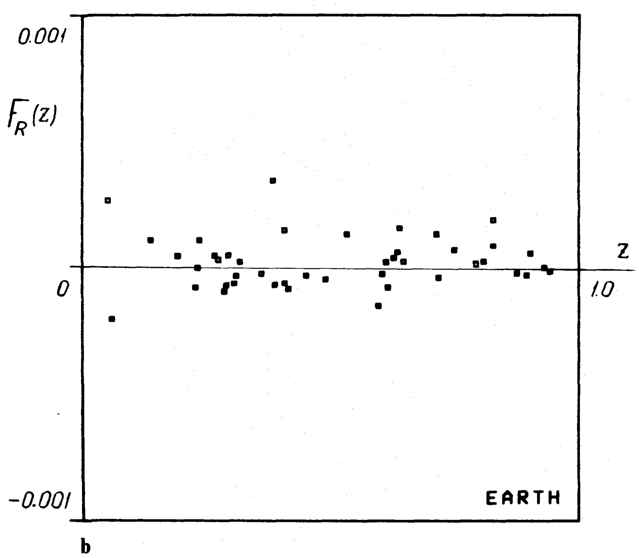

Fig. 2a–c. Comet Halley's perturbation by Jupiter (**a**), by Saturn (**b**), and residual perturbation (**c**). Curves are Fourier approximation (FA), straight lines are "saw-tooth" approximation (STA)

Hamiltonian of the system is periodic in all phases. Notice that in the presence of Saturn's perturbation one should either use the global phase $X_n(Y_n = r_S X_n)$ in map (3), as we did, or add the equation $y_{n+1} = y_n + r_S w_{n+1}^{-3/2}$.

In Fig. 2c the residual perturbation $F_R(z)$ is also plotted vs. phase of the Earth $z = Z(\text{mod } 1)$ where $Z = r_E X$, and $r_E = P_J$ (years) $= 11.86241$ is the Earth's frequency in the units adopted. We failed to find any simple dynamical interpretation for F_R which, therefore, characterizes the accuracy of our model (3):

$$\left(\frac{\langle F_R^2 \rangle}{\langle F_J^2 \rangle}\right)^{1/2} \approx 0.030; \quad \frac{\langle F_R^2 \rangle^{1/2}}{w} \approx 3.5\,10^{-4}; \quad \langle (\Delta t)^2 \rangle^{1/2} \approx 14 \text{ days} \tag{5}$$

Here Δt is the error in "prediction" of the next (or preceding) perihelion passage time.

In the process of successive approximations of F_J, F_S the parameters P_J and r_S as well as the number of Fourier harmonics have been also optimized by minimizing residual $\langle F_R^2 \rangle$. Interestingly, the optimizing proved to be very sensitive to the value of P_J so that the empirical uncertainty in this model parameter is only 0.01 days ≈ 15 min! Similarly, the relative uncertainty of effective frequency of Saturn r_S is $\sim 10^{-6}$.

The developed model (3), together with the empirical perturbation (Table 2), is of course nothing more than a physically meaningful interpolation of the original data t_n.

Besides the Fourier approximation (FA) of the perturbations we made also use of a simpler "saw-tooth" approximation (STA) where each of the functions $F_J(x)$, $F_S(y)$ was represented by the two straight lines as shown in Fig. 2. The amplitudes and vertex positions have been assumed as follows

$$A_J = 6.35\,10^{-3}; \quad x_+ = 0.552; \quad x_- = 0.640;$$
$$A_S = 1.05\,10^{-3}; \quad y_+ = 0.305; \quad y_- = 0.385;$$
$$2d_J = x_- - x_+ = 0.088; \quad 2d_S = y_- - y_+ = 0.080 \tag{6}$$

Naturally, the accuracy of the latter approximation is much worse [cf. Eq. (5)]:

$$\left(\frac{\langle F_R^2 \rangle}{\langle F_J^2 \rangle}\right)^{1/2} \approx 0.10; \quad \frac{\langle F_R^2 \rangle^{1/2}}{w} \approx 1.2\,10^{-3}; \quad \langle (\Delta t)^2 \rangle^{1/2} \approx 50 \text{ days}$$

We mention that the dynamics of 2-dim maps with a "saw-tooth" perturbation, similar to map (3), was studied before by Chirikov et al. (1971), and Chirikov and Izrailev (1976); see also Lichtenberg and Lieberman (1983) and Chirikov (1979).

A surprisingly sharp phase dependence of the perturbation (Fig. 2) is explained by relatively close encounters of the comet and planets due to a small inclination angle i of the orbit of the comet ($\sin i \approx 0.3$). Indeed, two encounters per turn are possible, both corresponding to approximately the same phases x and y. Recall that we define the perturbation phase at the perihelion passage time while the perturbation actually takes place at a different instant. The closest encounter corresponds to some "encounter phase" $x_c \approx 0.60$. Due to approximate symmetry of the encounter the value $F_J(x_c) \approx 0$. Saturn's encounter phase is $y_c \approx 0.35$.

Assuming the straight and uniform motion of both Jupiter and the comet at right angle to each other for a very close encounter ($\sin i \ll 1$, $d_J \ll 1$), the following simple analytical relation for the perturbation

$$-F_J(x) = \frac{2A_J(x-x_c)\,d_J}{(x-x_c)^2+d_T^2};$$

$$F_J(x_c)=0;$$

$$A_J = \frac{4\sqrt{2}}{3}\frac{\mu_J}{\sin i} \approx 0.0060;$$

$$d_J = \sqrt{\frac{3}{2}}\frac{\sin i}{2\pi} \approx 0.059 \tag{7}$$

can be shown to hold within some interval around x_c including both $|F_J|$ maxima. Numerical values are given for comet Halley. They agree quite well with Eqs. (6), and do so still better with a more accurate FA presented in Fig. 2a which gives $A_J \approx 0.0059$ and $d_J \approx 0.062$. Notice, however, that the empirical function $F_J(x)$ is slightly asymmetric with respect to phase $x_c \approx 0.60$.

For Saturn's perturbation only the values of phase y_c and of amplitude A_S in Eq. (7) change, namely

$$\frac{A_S}{A_J} = \frac{\mu_S}{\mu_J a_S} = 0.163 \tag{8}$$

where μ_S, a_S are the mass and radius of the orbit of Saturn. The data in Fig. 2 give $A_S/A_J \approx 0.175$.

Other planets as well as the nongravitational forces (see Yeomans and Kiang, 1981; Landgraf, 1986) yield a perturbation comparable with the residual one (5): $(\langle F_\Sigma^2\rangle | \langle F_J^2\rangle)^{1/2} \approx 0.025$ (Chirikov and Vecheslavov, 1986). The latter includes, of course, the effect of some other model approximations, particularly, the assumed circular orbits of Jupiter and Saturn.

At small w the perturbation $F(x)$ is nearly independent of w [see Eq. (7)] as the energy exchange with Jupiter is determined by the "local" (osculating) speed of the comet $v^2 \approx 2 \gg w$. This was the reason to choose the quantity w as a dynamical variable of our model.

3. Local instability of motion

A strong local instability of motion – the exponential divergence of close trajectories – is commonly accepted by now as the simplest and most reliable criterion for dynamical chaos, at least, in numerical experiments (Lichtenberg and Lieberman, 1983; Zaslavsky, 1985; Chirikov, 1979). We studied this instability via the linearized equations of model (3) (for Jupiter's perturbation only):

$$\delta w_{n+1} = \delta w_n + F'(x_n^0)\delta x_n,$$

$$\delta x_{n+1} = \delta x_n - \tfrac{3}{2}(w_{n+1}^0)^{-5/2}\delta w_{n+1}, \tag{9}$$

where (x_n^0, w_n^0) is a reference trajectory, and $(\delta x_n, \delta w_n)$ the tangent vector $\boldsymbol{l}$. The nature of the dynamics of vector $\boldsymbol{l}$ is determined by the Lyapunov exponent

$$\Lambda \approx \frac{1}{n}\ln\frac{l_n}{l_0}, \quad n\to\infty \tag{10}$$

For a 2-dim. map $\Lambda = h$, the Kolmogorov-Sinai entropy. Dynamical chaos occurs under the conditions $h>0$, or $\Lambda>0$.

The eigenvalues of matrix (9) satisfy the condition $\lambda_1\lambda_2=1$. Denote the largest eigenvalue modulus by λ_n; it depends on the iteration serial number n. Then:

$$\ln\lambda_n = |\ln|1-k_n+\sqrt{k_n^2-2k_n}||;$$

$$k_n = \tfrac{3}{4} w_{n+1}^{-5/2} F'(x_n), \tag{11}$$

where we drop the superscript zero for the reference trajectory. In the STA (6)

$$k_n = \begin{cases} -\dfrac{0.108}{w_n^{5/2}}; & 0.552 < x_n < 0.640 \\[2mm] \dfrac{0.0104}{w_n^{5/2}}; & \text{otherwise} \end{cases} \tag{12}$$

At the present value $w_n = w_1 \approx 0.3$, the instability occurs only within the phase interval given in the first line of Eq. (12) around encounter phase $X_c \approx 0.60$ where $\lambda_n \approx 6.2$. We shall call these phases unstable. For other x values $\lambda_n = 1$. Using Eqs. (11) and (12) we conclude that for

$$w_n < w_{cr} \approx 0.12 \tag{13}$$

all the phases become unstable as $|k_n| > 2$. In this domain there is a single solid chaotic component of motion. By contrast, at $w > w_{cr}$ large regions of stable motion arise around the fixed points of map (3):

$$w = w_m \approx m^{-2/3}; \quad x = x_f, \; F_J(x_f) = 0, \quad F_J'(x_f) > 0,$$

with m any integer (Fig. 3a). The oscillation period about a fixed point $P_m \approx 2\pi m^{1/6}[(1-2d_J)/3A_J]^{1/2} \approx 700$ yr (in STA). Remnants of this periodicity persist in the chaotic component. Apparently, they were noticed and discussed in Yeomans and Kiang (1981),

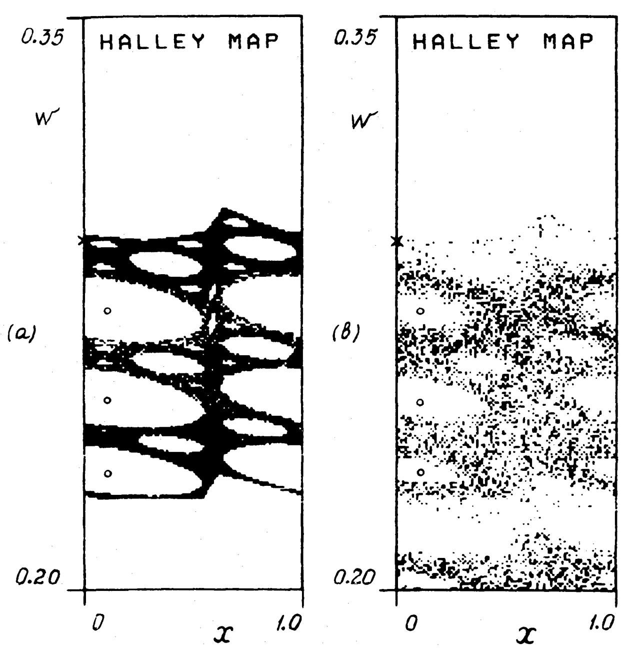

Fig. 3a and b. Phase trajectory of map (3) in the STA (6). Initial conditions (crosses) $w_1 = 0.29164$; $x_1 = 0$ (in 1986, see Table 1): **a** Jupiter's perturbation only, $N = 1.5\ 10^5$ iterations; **b** perturbation by both Jupiter and Saturn, $N = 4000$

Kiang (1979). There are fixed points at phase x_c (7) as well, yet all the latter are unstable since $F'_J(x_c)<0$.

In region $w>w_{cr}$ the motion instability grows only within the narrow interval of unstable phases (12). Let $p(w)$ be the probability for a trajectory to enter this unstable phase interval. Numerical simulation at $w\approx0.3$ gives: $h\approx0.26$ and $p\approx0.19$. Notice that the probability p considerably exceeds the interval width $2d_J=0.088$ (6). This is explained by a decrease in the area of the chaotic component outside of the unstable phase interval due to large stable regions there (Fig. 3a).

The motion of the comet changes substantially if Saturn's perturbation is "switched on" (Fig. 3b). Notice that upon including Saturn's perturbation the phase plane point (x, w) does no longer completely determine the trajectory which now also depends on Saturn's phase y. In other words, the plane in Fig. 3b is a 2-dim. projection of the 3-dim. phase space of map (3) (see Sect. 2). With Saturn's perturbation included, the stability domains decrease noticeably but persist. This leads to a reduction of the probability to $p\approx0.13$ and, consequently, of the entropy to $h\approx0.16$ while the unstable eigenvalue $\lambda\approx6.2$ remains nearly constant. The latter is explained by a weak influence of Saturn upon parameter k in Eq. (11).

By contrast, the perturbation caused by the Earth, being relatively weak, completely dominates nevertheless, upon a close encounter with the comet as the perturbation is concentrated within a very narrow interval of Earth's phase z. Destabilizing effects of close encounters with the Earth are well known from numerical simulation of cometary trajectories (Yeomans and Kiang, 1981; Brady and Carpenter, 1971; Landgraf, 1986). However, the Earth's contribution to the entropy is insignificant (Chirikov and Vecheslavov, 1986).

Within stability domains the motion is quasiperiodic, i.e. of a discrete spectrum, and the w variation is strictly bounded and small, while entropy $h=0$. Interestingly, the present value of comet Halley's energy is only 3% above the nearest stability region. However, the residual perturbation F_R makes the existence of such regions questionable.

4. The error factor in numerical simulations of a chaotic trajectory

The local instability of comet Halley's motion is the cause of its chaotic behaviour, particularly, of the diffusion in energy (Sects. 5, 6). Moreover, the instability sharply restricts any extrapolation of the comet's trajectory both forward and backward in time. The most error-sensitive quantity is the perihelion passage time t_n or the perturbation phase x_n. Just those t_n errors are given usually in the papers on numerical simulations of the comet's dynamics (Yeomans and Kiang, 1981; Kalyuka et al., 1985; Brady and Carpenter, 1971; Landgraf, 1986). On the other hand, x_n errors significantly change the motion of the comet as the trajectory may pass from stable to unstable phases and vice versa. Define the error factor

$$f_m=\left|\frac{\delta x_m}{\delta x_0}\right| \tag{14}$$

which describes the growth of phase errors over m revolutions of the comet.

For $m\gg1$ the mean error factor relates to the entropy (Sect. 3):

$$\bar{f}_m\approx e^{hm}. \tag{15}$$

Assume the largest tolerable error $|\delta x_m|$ to be of the order of $d_J\sim0.05$, $|\delta t_m|\sim200$ days [a half-width of the unstable phase interval, see Eq. (6)]. Then, the extrapolation is restricted to

$$N_{\text{ext}}\approx\frac{1}{h}\ln\frac{d_J}{|\delta x_0|}\approx-6.3\ln|\delta x_0|-19 \tag{16}$$

It grows only logarithmically with the modelling accuracy $|\delta x_0|$. In Eq. (16) we use the value $h=0.16$. Assuming an effective initial error $|\delta x_0|\approx5\,10^{-4}$, $|\delta t_0|\approx2$ days (see below) we obtain $N_{\text{ext}}\approx29$ revolutions.

This estimate is rather crude, due to big fluctuations during relatively short times, particularly, because of a narrow interval of unstable phases. A more accurate evaluation of the error factor can be performed as follows.

Consider the linearized map (9) on some interval (t_n, t_m) using the "true" orbit (Table 1) as reference trajectory. Then, the error factor can be estimated, within this interval, as the biggest eigenvalue modulus of the corresponding transfer matrix $f_{n,m}\sim\lambda_{n,m}$. The quantity $(\ln\lambda_{n,m})/(m-n)=h_{n,m}$ describes a "current" entropy on this interval (t_n, t_m). For instance, $h_{4,46}=0.24$, which noticeably exceeds the mean value $h=0.16$. The latter is reached in a longer time interval. The former value may be compared to $h=0.30$ as measured by means of maps (3) and (9) (Sect. 3) for 50 revolutions of the comet.

As the errors of the linearized map also grow exponentially, the transfer matrix is better evaluated by multiplying the matrices of each iteration rather than numerically iterating map (9).

As a particular example we estimate the extrapolation accuracy for comet Halley's trajectory in Yeomans and Kiang (1981). The main parameters of this trajectory were determined from apparitions of the comet in 1759, 1682 and 1607. However, the most error-sensitive quantity t_n was set to the observational value in 837 ($n=16$). So we assumed just the latter date as the beginning of the extrapolation in evaluating $\lambda_{16,m}$. These values are depicted

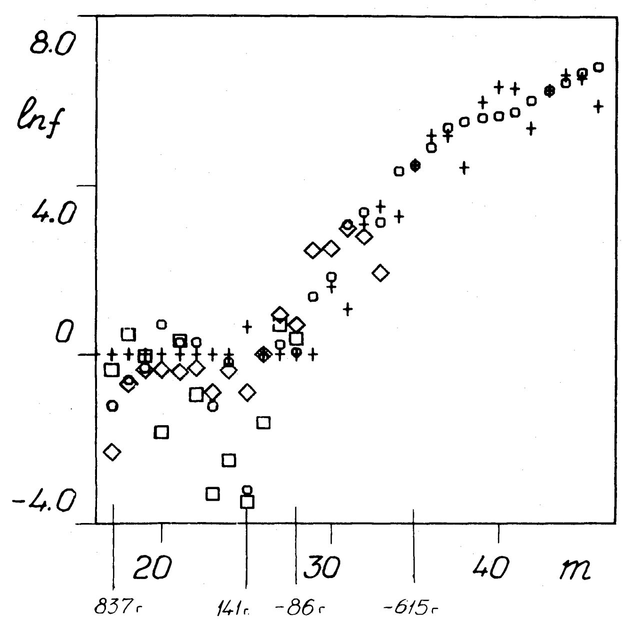

Fig. 4. Error factor f in extrapolation of comet Halley's chaotic trajectory (in 837 through -1403). Dependence of $\ln(|\delta t_m|/\delta t_{\text{in}})=\ln f$ vs. $m=17$–46 is shown after Yeomans and Kiang, 1981 (squares); Landgraf, 1986 (diamonds); our model (3) (circles), and $\ln\lambda_{16,m}$ (crosses), see text

in Fig. 4 for $m=17-46$ (crosses) which correspond to the extrapolation back to -1403 in Yeomans and Kiang (1981). A peculiar feature of this dependence is a rather long interval of stable motion ($\lambda=1$, $m=17-29$ except $\lambda_{16,25}=1.89$) followed by a fairly steep instability. It is important to note that the earliest reliable observations of comet Halley fall just on the stable interval (in -86, $m=28$, Yeomans and Kiang (1981)). The previous apparition in -163 ($m=29$) dated to some accuracy in Stephenson et al. (1985), is located near the beginning of unstable region (see Fig. 4). In other words, the proper extrapolation, in absence of any observational data, gets actually into the unstable part of the trajectory. At the end of the extrapolation the error factor amounts to $f_{16,44} \sim \lambda_{16,44} \approx 700$.

As the initial error δt_{in} it is natural to assume the rms deviation of the computed t_m from their observational values within the stable interval $m=17-28$. Using the data of Table 5 in Yeomans and Kiang (1981) we find $\delta t_{\mathrm{in}}=2.7$ days. At the end of extrapolation interval the error $|\delta t_{44}| \approx \delta t_{\mathrm{in}} f_{16,44} \sim 5$ yr becomes prohibitively large. The extrapolation holds, therefore, only up to about $m=35$ (in -615) when $|\delta t_{35}| \sim 200$ days.

As a check of these estimates we made a similar extrapolation with our model (3) in the FA with the perturbation by Saturn included. We have slightly corrected the value w_{16} in order to decrease δt_{25} (in 141) as well as it had been done in Yeomans and Kiang (1981). Actually, the eccentricity was corrected there but, curiously, both relative changes proved to be very close: $|\Delta\varepsilon|/(1-\varepsilon) \approx |\Delta w|/w \approx 2.2\ 10^{-4}$. The initial error for our model, calculated in the same way as above, $\delta t_{\mathrm{in}} \approx 19$ days, is in a reasonable agreement with the rms accuracy (5), and is only 7 times the error in Yeomans and Kiang (1981). The model values of $\ln(|\delta t_m|/\delta t_{\mathrm{in}})$ are represented in Fig. 4 by circles, and they clearly demonstrate a "sudden" burst of instability. Our analysis explains a surprise strong divergence of different extrapolations of the orbit of comet Halley prior to -86 presented recently by Stephenson et al. (1985) (see their Fig. 2).

Finally, one may compare trajectory of the comet in Yeomans and Kiang (1981) with the recent computation in Landgraf (1986), Table 8, sample I, for instance. The result is shown in Fig. 4 by diamonds. The rms difference between the two trajectories within the stable section is $\delta t_{\mathrm{in}}=0.9$ day. At the end of the extrapolation of the trajectory in Landgraf (1986) the error factor reaches the value $f_{16,33} \sim \lambda_{16,33} \approx 30$, and the separation of the trajectories becomes $|\delta t_{33}| \sim 27$ days. Why in the final version of trajectory of the comet as presented in Table 9 in Landgraf (1986) the same separation lies within about one day remains a mystery for us.

In any event, all the above data definitely point out a rapid growth of the extrapolation errors in the time interval under consideration. This may explain some difficulties in reconciling the observational data in -465 and -617 with extrapolated trajectories of comet Halley as mentioned in Landgraf (1986).

We emphasize that the error growth in our model relates to the perturbation by Jupiter (and Saturn) only, without any contribution from the Earth, which would increase the errors still more. We mention that the instability of the motion and the growth of the error in a simple three-body model were noticed in Kiang (1979) and certainly follow from the results of Petrosky (1986).

For comparison we note that the computational accuracy for the stable (quasiperiodic) motion of planets in the solar system on the same time interval is equivalent to $\delta t \sim 1$ day, and weakly depends on time (see, e.g. Table 2 in Yeomans and Kiang, 1981).

Contrary to the extrapolation, the interpolation of a chaotic trajectory gives much more accurate results. Particularly, it is demonstrated by surprisingly small errors of our fairly simple model (3). How strange it may seem at first glance, the interpolation is the simpler (requires the less changes in initial conditions and/or system parameters) the stronger the local instability of motion is. It is the property of structural stability (robustness) of chaotic dynamics which also provides stability of the statistical description.

Notice that big absolute errors of t_n for the computed trajectory of the comet in Yeomans and Kiang (1981) do not prevent us from using this trajectory for the reconstruction of the perturbation $F(x)$ in Sect. 2. The point is that we need three successive values t_n only, and the reconstruction accuracy depends on trajectory errors within two revolutions of the comet.

5. The local diffusion rate of a chaotic trajectory

Within a chaotic component of the motion of a comet, the perturbation $F(x)$ causes a diffusion in w. If perturbation phases x_n would not only be random (which they are due to the local instability) but also statistically independent (which they generally are not in spite of randomness) then the diffusion rate would be determined simply by the mean square of the perturbation (see, e.g., Lichtenberg and Lieberman, 1983; Zaslavsky, 1985):

$$D \equiv \frac{\langle (\Delta w)^2 \rangle}{m} = D_0 = \langle F^2(x) \rangle \approx \frac{A_J^2}{3} \approx 1.3\ 10^{-5} \tag{17}$$

That limiting case holds at $w \ll w_{\mathrm{cr}}$ when all the phases are unstable (Sect. 3). Here Saturn's contribution is negligibly small ($A_S^2/A_J^2 \approx 0.03$).

As w grows, the entropy drops (11) which results in a time correlation, and in diffusion deceleration. This becomes especially significant for $w > w_{\mathrm{cr}}$ due to the formation of domains with a regular motion (Fig. 3). This is just the case for the present value $w_1 \approx 0.3$.

We numerically measured the local (a small change in w) diffusion rate by averaging over 1024 trajectories of 46 iterations each with slightly different initial conditions. In the FA the rate $D(w_1) \approx 5.6\ 10^{-6}$, while the STA gives $6.0\ 10^{-6}$. It is about two times less than D_0 (17). "Switching-off" Saturn's perturbation somewhat decreases the diffusion ($4.4\ 10^{-6}$) due to a stronger correlation. A residual perturbation F_R (Sect. 2) in the form of a random noise with the same rms magnitude does not change the rate: $5.5\ 10^{-6}$ (FA).

Finally, we directly used the data of Table 1 in Yeomans and Kiang (1981), which is equivalent to one trajectory in the previous method. It gives a close value of $7.4\ 10^{-6}$.

We also mention that for larger w the diffusion rate drops, e.g., $D(0.7) \approx 2.7\ 10^{-6}$.

6. Global dynamics of comet Halley

The simple model (3) does not take any other orbit parameters into account besides w, and therefore its straightforward application is restricted by a relatively short time interval.

The most significant effect seems to be a periodic crossing of Jupiter's and the comet's orbits due to the perihelion precession with a period $N_p \approx 440$ revolutions of the comet (see Yeomans and Kiang, 1981). This leads to a considerable decrease of the minimal Jupiter-comet distance s as compared to the present value

$s_1 = \sin i \approx 0.3$. As a result, the prompt ejection of the comet out of the solar system may happen in a single very close encounter with Jupiter. A rough estimate for the ejection mean life time of the comet

$$N_{ej} \approx \frac{\pi}{2d_J}\left(\frac{w}{A_J}\right)^2 \approx 10^5 \qquad (18)$$

turns out to be surprisingly long, well in excess of the diffusion life time (see below). We mention that the probability for the comet to drop on Jupiter is still about 100 times lower. On the other hand, the diffusion rate remains of the same order in spite of the crossing of the orbits (Chirikov and Vecheslavov, 1986).

Another omitted effect, which is important for the global dynamics, is apparently the diffusion in inclination i, as perturbation $F(x) \propto (\sin i)^{-1}$ (7). A rough estimate, obtained from the data in Yeomans and Kiang (1981), Table 4 (see Chirikov and Vecheslavov, 1986) shows that even though the diffusion in i can hardly be neglected completely it does not seem to change the order of magnitude for life time of the comet in the solar system, especially in view of big fluctuations of the latter (see below).

In the STA a connected chaotic component is unbounded in w because of a slow decay of the Fourier harmonics of the perturbation (Chirikov, 1979; Chirikov et al., 1971; Chirikov and Izrailev, 1976). For the true smooth perturbation, the chaotic component is limited from above: $w < w_b$. Yet, the limit is much higher than $w_1 \approx 0.3$, and therefore is unimportant here. Numerical simulation shows that, at any rate, $w_b > 0.6$, $P_b < 25.5$ yr. What is important is that the chaotic component extends down to $w = 0$, i.e. the comet leaves eventually the solar system along a hyperbolic orbit.

In the independent-phase approximation (17) the diffusion life time of the comet would be

$$N_D \sim \frac{w^2}{D_0} \approx \frac{3w^2}{A_J^2}, \qquad (19)$$

which is much shorter than the ejection life time: $N_D/N_{ej} \approx 2d_J \approx 0.1$. Notice, that even though Eq. (18) for N_{ej} has a "diffusion appearance" it is not necessarily related to any chaotic motion, and it holds for regular trajectories as well provided the phase x varies over the whole interval, i.e. is rotating.

The diffusion proceeds down to $w_{min} \sim A_J \approx 0.006$ which corresponds to the comet's period $P_{max} \sim 2.6\ 10^4$ yr, and to its aphelion $2a_{max} \sim 1700$ AU.

We carried out numerical simulations of the global dynamics using 40 trajectories of map (3) with initial conditions from Table 1. Because of the local instability all these trajectories rapidly diverge and show quite different values of the life time:

$$1374 \leqslant N_D < 10^5; \quad 5.3\ 10^5 \leqslant t_D(\text{years}) \leqslant 2\ 10^7.$$

The scattering is due to big diffusion fluctuations, especially, at $w > w_{cr}$. An example of the full phase trajectory, projected onto plane (x, w), is depicted in Fig. 5a.

The mean diffusion life time of the comet is equal to

$$\bar{N}_D \approx 1.8\ 10^4; \quad \bar{t}_D \approx 3.9\ 10^6 \text{ years}$$

the average period being $\bar{P}_D = \bar{t}_D/\bar{N}_D \approx 220$ yr, and the mean rate of global diffusion $\bar{D}_G \approx w_1^2/\bar{N}_D \approx 5\ 10^{-6}$. The latter is close to the local diffusion rate (Sect. 5).

The global diffusion primarily proceeds downwards in w because of the increase of $D(w)$ in this direction.

The comet's life time, unlike the local diffusion rate, crucially depends on a relatively weak perturbation by Saturn. If it is

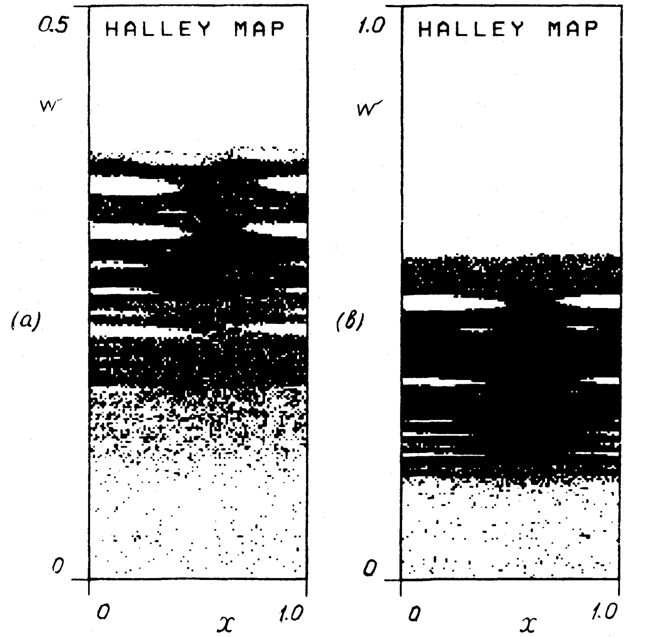

Fig. 5a and b. Two examples of comet Halley's global dynamics in model (3), $N_D \approx 4.1\ 10^4$, $t_D \approx 4.5\ 10^6$ yr (**a**); with a variable nongravitational acceleration (20), $\bar{F} = 3\ 10^{-5}$, $N_{ev} = 10^3$, $\tilde{N}_{Dd} \approx 3.1\ 10^5$, $\tilde{t}_{Dd} \approx 2.1\ 10^7$ yr (**b**)

"switched-off", the life time jumps up to $\bar{N}_D \approx 6\ 10^5$ ($\bar{t}_D \approx 6\ 10^7$ yr), i.e. by a factor of 20, due to a long-time "sticking" of the trajectory in some narrow w layers. Under these circumstances even a weak additional perturbation may greatly change the life time. Notice that the comet's mean period $\bar{P}_D \approx 100$ yr remains close to the initial $P_1 \approx 76$ yr.

As the diffusion proceeds symmetrically in both directions of time, the full sojourn time of the comet in the solar system is twice as big, $2\bar{N}_D$. Certainly, the comet's actual life time may be determined by totally different physical processes, for example, simply by its evaporation. Recent data in Boyarchuk et al. (1986) indicate that the evaporation time may be as short as $N_{ev} \approx 4000$ revolutions. However, there is no such limitation backwards in time.

Another important effect is a systematic variation of w (a drift). The physical cause of the drift is the so called transverse nongravitational acceleration (force) related to evaporation of cometary material near the Sun (Marsden et al., 1973). Using the latest data on the parameters of non-gravitational forces (Kalyuka et al., 1985; Landgraf, 1986) we find

$$\overline{\frac{dw}{dn}} = \overline{F(x)} \approx +3\ 10^{-5}$$

backward in time. Forward in time $\bar{F} < 0$ which would result in the comet leaving the solar system after about $N_d \approx w_1/\bar{F} \approx 10^4$ revolutions, that is somewhat faster than $\bar{N}_D \approx 1.8\ 10^4$. The combination of both diffusion and drift would decrease the life time still further; numerically, $\bar{N}_{Dd} \approx 6600$.

We mention that the change of phase volume (dissipativity), which is inevitably related to the drift, is, nevertheless, much smaller, so that the corresponding time N_{dis} can be shown to have the order $N_{dis}/N_d \sim (qw)^{-1} \sim 30$ where $q \approx 0.6$ AU ≈ 0.12 is the comet's perihelion distance. Hence, map (3) can be treated as a canonical one even in the presence of drift.

The effect of the drift is much stronger backward in time ($\bar{F}>0$). In this case the variation of w is eventually determined by the drift only, that is w continuously grows after some time because of a sharp decrease in the diffusion rate with w (Sect. 5).

Now, we take into account a possible time-variation of the nongravitational forces. For example, evaporation would cause the comet's mass to decrease thereby increasing the nongravitational acceleration. A natural time scale for that process would be the evaporation time of $N_{ev} \approx 4000$ revolutions of the comet (Boyarchuk et al., 1986). Because of this we modified the drift equation as follows (backward motion, $\bar{F}>0$):

$$\overline{\frac{dw}{dn}} = \frac{\bar{F}}{1+\frac{n}{N_{ev}}} = \tilde{F}(n). \tag{20}$$

The decrease of the drift speed $\tilde{F}$ with n leads eventually to a purely diffusive motion. Yet, the life time of the comet increases considerably as compared to that without drift. This is because the drift, decreasing though, still leaves enough time for the comet to move to a bigger w where the diffusion rate sharply drops (Sect. 5).

According to numerical simulations, the life time for Eq. (20) is $\tilde{N}_{Dd} \gtrsim 5\ 10^5$. Even upon reducing N_{ev} to 10^3, the mean life time $\tilde{N}_{Dd} \approx 1.4\ 10^5$ is still much longer than $\bar{N}_D \approx 1.8 \times 10^4$. An example of the latter trajectory with $\tilde{N}_{Dd} = 3.1\ 10^5$ is given in Fig. 5b. Under these circumstances the variation of the inclination i as well as the single ejection of the comet by Jupiter (18) may play an important role. Even though the models of nongravitational forces used above, especially Eq. (20), remain highly hypothetical, it is completely clear from our numerical simulations that their impact on the global dynamics and life time of comet Halley is crucial.

7. Conclusion

A fairly simple model for the comet Halley's dynamics, developed in the present paper, allows to study essential features of its short- and long-term evolution in both directions of time. Numerical simulations as well as the analytical calculations reveal that the motion of the comet is chaotic, and allow to evaluate the error growth in the extrapolation of its trajectory. We would like to emphasize again that the mean error growth is determined primarily by Jupiter's perturbation, and not by the comet's encounters with the Earth which seems to be a common belief (see, e.g. Yeomans and Kiang, 1981; Landgraf, 1986). Also, for any chaotic trajectory the mean error growth in time is exponential but not a power law one as is sometimes assumed. Increasing the computational accuracy helps, therefore, only on a short time interval as is easily verified by a slight change in initial conditions or by the time reversal.

The chaotic (non-periodic) nature of the motion is one of its important characteristics, and we propose to mark it by a special letter C (e.g. C/Halley instead of P/Halley) as a warning against underestimation of the errors in extrapolation of the chaotic trajectory.

Since chaotic motion has a continuous temporal Fourier spectrum, the so called "cyclic method", i.e. the search of commensurabilities in motions of the comet, Jupiter and Saturn (Kamieńsky, 1962) is totally inapplicable here. This highlights the qualitative distinction of chaotic motion from a regular (quasi-periodic) one, as the motion of the planets, for example, where this method is successfully used. We remind the reader that the perturbation in our model is a regular (quasiperiodic) function of time.

Dynamical chaos results in the diffusion of the orbit of comet in both directions of time, so that the comet is found eventually outside of the solar system. Numerical simulations show that the sojourn time of comet Halley within the solar system crucially depends on weak nongravitational forces acting upon the comet near the Sun. Interestingly, repeated crossings between the orbits of the planets and the comet only insignificantly affect the life time of the comet. The estimated sojourn time of comet Halley in the solar system ($N \sim 10^5$; $t \sim 10^7$ years) turns out to be much smaller then cosmological time scale which poses a serious problem related to the origin of comets. In this connection we would like to attract attention to the fact that the above time is of the same order of magnitude as the period of hypothetical comet showers from the Oort cloud conjectured recently in Hut et al. (1987).

Acknowledgements. We acknowledge interesting discussions with F.M. Izrailev and D.L. Shepelyansky as well as helpful comments and suggestions from M. Grewing, C.D. Murray and D.K. Yeomans.

References

Arnold, V.I.: 1964, *Dokl. Akad. Nauk SSSR* **156**, 9
Boyarchuk, A.A., Grinin, V.P., Zvereva, A.M., Petrov, P.P., Sheihet, A.I.: 1986, *Astron. Zh.* (Pisma) **12**, 696
Brady, J.L., Carpenter, E.: 1971, *Astron. J.* **76**, 728
Chirikov, B.V.: 1979, *Phys. Reports* **52**, 263
Chirikov, B.V., Keil, E., Sessler, A.M.: 1971, *J. Stat. Phys.* **3**, 307
Chirikov, B.V., Izrailev, F.M.: 1976, in *Colloques Intern. du CNRS*, N 229 (Toulouse, 1973), Paris, p. 409
Chirikov, B.V., Vecheslavov, V.V.: 1986, preprint INP 86-184, Novosibirsk, USSR
Everhart, E.: 1979, in *Asteroids*, Arizona
Froeschlé, C., Scholl, H.: 1981, *Astron. Astrophys.* **93**, 62
Gontkovskaja, V.T., Chebotarev, G.A.: 1964, *Astron. Zh.* **XXXVIII**, N 1, 125
Hut, P., Alvarez, W., et al.: 1987, *Nature* **329**, 118
Kalyuka, Yu.F., Tarasov, V.P., Tikhonov, V.F.: 1985, *Astron. Zh.* (Pisma) **11**, 788
Kamieński, M.: 1962, *Acta Astron.* **12**, 227
Kiang, T.: 1979, in *Dynamics of the Solar System*, IAU Symp., N 81, Dordrecht, Holland, p. 303
Landgraf, W.: 1986, *Astron. Astrophys.* **183**, 246
Lichtenberg, A.J., Lieberman, M.A.: 1983, *Regular and Stochastic Motion.* Springer, Berlin, Heidelberg, New York
Marsden, B.C., Sekanina, Z., Yeomans, D.K.: 1973, *Astron. J.* **78**, 211
Petrosky, T.Y.: 1986, *Phys. Lett.* **A117**, 328
Sagdeev, R.Z., Zaslavsky, G.M.: 1987, *Nuovo Chimento* **97B**, N 2, 119
Stephenson, F.R., Yau, K.K.C., Hunger, H.: 1985, *Nature*, **314**, 587
Wisdom, J.: 1980, *Astron. J.* **85**, N 8, 1122
Wisdom, J., Peale, S., Mignard, F.: 1983, *Icarus* **58**, 137
Yeomans, D.K., Kiang, T.: 1981, *Monthly Notices Roy. Astron. Soc.* **197**, 633
Zaslavsky, G.M.: 1985, *Chaos in Dynamical Systems*, Harwood, New York